The American Journal of Pathology, Vol. 169, No. 4, October 2006

DOI: 10.2353/ajpath.2006.051333

Molecular Pathogenesis of Genetic and Inherited Diseases

Impact of the Loss of *Hoxa5* Function on Lung Alveogenesis

Isabel Mandeville,* Josée Aubin,* Michelle LeBlanc,* Mélanie Lalancette-Hébert,* Marie-France Janelle,† Guy M. Tremblay,† and Lucie Jeannotte*

From the Centre de Recherche en Cancérologie de l'Université Laval, Centre Hospitalier Universitaire de Québec, Québec; and the Centre de Recherche de L'Hôpital Laval,† Institut de Cardiologie et de Pneumologie de l'Université Laval, Québec, Québec, Canada*

The involvement of genes controlling embryonic processes in the etiology of diseases often escapes attention because of the focus given to their inherent developmental role. *Hoxa5* belongs to the *Hox* gene family encoding transcription factors known for their role in skeletal patterning. *Hoxa5* is required for embryonic respiratory tract morphogenesis. We now show that the loss of *Hoxa5* function has severe repercussions on postnatal lung development. *Hoxa5*$^{-/-}$ lungs present an emphysema-like morphology because of impaired alveogenesis. Chronic inflammation characteristics, including goblet cell hyperplasia, mucus hypersecretion, and recruitment of inflammatory cells, were also observed. Altered cell specification during lung morphogenesis triggered goblet cell anomalies. In addition, the defective motility of alveolar myofibroblast precursors in the embryonic lung led to the mispositioning of the alveolar myofibroblasts and to abnormal elastin deposition postnatally. Both goblet cell hyperplasia and elastic fiber abnormalities contributed to the chronic physiopathological features of *Hoxa5*$^{-/-}$ lungs. They constituted an attractive stimulus to recruit activated macrophages that in turn generated a positive feedback loop that perpetuated macrophage accumulation in the lung. The present work corroborates the notion that altered *Hox* gene expression may predispose to lung pathologies. *(Am J Pathol 2006, 169:1312–1327; DOI: 10.2353/ajpath.2006.051333)*

Lung morphogenesis relies on finely orchestrated processes that initiate from the outpocketing and the elongation of the foregut endoderm into the surrounding mesenchyme. The lung bud then branches extensively giving rise to saccules that expend and subdivide to ultimately produce alveoli. In the mouse, the main stem bronchi form at approximately embryonic day (E) 9.5, and ramification organized by signaling centers shapes the respiratory tree during the pseudoglandular period that extends from E14.0 to E16.5. At late gestational stages, saccules are found at the end of each terminus of the pulmonary tree. The last step of lung morphogenesis occurs between postnatal day (P) 5 and P30, and it aims at multiplying the respiratory surface for vital gas exchanges after birth by modifying the distal lung architecture through the process of alveogenesis. During each step of lung development, the concerted action of transcriptional regulators, signaling molecules, their associated receptors and downstream effectors governs branching morphogenesis and lung maturation by integrating cellular proliferation, differentiation, apoptosis, and migration.[1–3] Proper expression of these factors is further required to maintain pulmonary homeostasis.

Impairment of any step of lung morphogenesis and maturation can cause pathologies and compromise viability. Beside premature death at birth, impaired lung development and maturation can lead to consequences similar to those observed in multiple pulmonary disorders resulting from inflicted alveolar damages, such as chronic obstructive pulmonary disease (COPD). This complex pathology stems from a chronic inflammatory process coupled to goblet cell hyperplasia and mucus hypersecretion.[4,5] As well, emphysema, which is a major component of the morbidity and mortality of COPD, is defined as the enlargement of peripheral airspaces because of the destruction of alveolar septas.[6] Mouse molecular genetics have provided important insights into the regulatory networks underlying lung morphogenesis and

Supported by the Canadian Institutes of Health Research (grant MOP-15139 to L.J.) and the Fonds de la Recherche en Santé du Québec (Chercheur National Award to L.J.).

I.M., J.A., and M.L. contributed equally to this work.

Accepted for publication June 27, 2006.

Address reprint requests to Lucie Jeannotte, Centre de Recherche de L'Hôtel-Dieu de Québec, 9, rue McMahon, Québec, QC, Canada, G1R 2J6. E-mail: lucie.jeannotte@crhdq.ulaval.ca.

pathology. For instance, the loss of *Pdgfa* gene function perturbs alveolar septation, which results in lungs with an emphysema-like appearance.[7] *Pdgfa*$^{-/-}$ surviving mice are missing alveolar smooth muscle cells, which contribute to elastin deposition during alveogenesis.[8,9] Accordingly, the amount of lung elastin is reduced in these mutants. Elastin constitutes the most abundant extracellular matrix component in the lung, participating in the elastic fibers that allow the tissue to stretch and recoil without damage during respiration.[10] Deposition of elastin by alveolar myofibroblasts is coupled to alveolar septation and critical for distal airway branching.[11–13]

Lung formation relies on several transcription factors including the proto-oncogene *N-myc*, forkhead domain proteins such as Foxa2, and homeobox-containing proteins.[3,14,15] Expression of some key regulators of lung embryonic development persists through adulthood, suggesting that they may participate in postnatal alveogenesis. For instance, Foxa2 regulates several genes involved in lung morphogenesis and homeostasis, such as *Nkx2.1*,[16] *Sftpb* (coding for surfactant protein B; SP-B),[17] and *Muc5ac* (coding for mucin MUC5AC).[18] *Foxa2* also takes part in alveogenesis because its specific deletion in airway epithelial cells results in airspace enlargement. The loss of *Foxa2* function further causes goblet cell hyperplasia and increased mucus production, pathological features commonly associated to chronic respiratory diseases in humans.[18]

Although much emphasis has initially been focused on their role in skeletal patterning, the *Hox* gene family also serves essential functions in the elaboration of organs as evidenced by the variety of defects encountered in *Hox* mutant mice.[19] This family comprises 39 members clustered in four complexes, each located on a different chromosome. Approximately 20 *Hox* genes, predominantly from paralogous groups 2 to 6, are expressed in the lung, where they display a distinct spatio-temporal pattern of expression.[14,20] Despite the fact that mutant mouse lines for several lung-expressed *Hox* genes have been generated, the consequences on respiratory tract development and function have been examined for a limited number of these. Although the *Hoxa1* mutation does not affect lung development per se, it results in perinatal death caused by anoxia, a problem due to defective hindbrain patterning.[21] The combined mutation of the *Hoxa1* and *Hoxb1* genes results in hypoplastic lungs with a reduced number of lobes but a normal histology, implying some functional redundancy between *Hox1* paralogs during lung formation.[22] The *Hoxa3* gene participates to the patterning of the proximal airways, more specifically to the development of the larynx.[23] Although no lung phenotype has been reported in *Hoxb5*$^{-/-}$ mice,[24] abnormal *Hoxb5* expression correlates with alterations in bronchiolar branching.[25] Moreover, the *HOXB5* gene was found aberrantly expressed in patients suffering from bronchopulmonary sequestration and congenital cystic adenomatoid malformation.[26]

The analysis of the *Hoxa5* mutant mouse line has revealed the preponderant role of this gene in lung development and maturation.[27,28] The loss of *Hoxa5* function severely compromises viability at birth because of tracchea and lung dysmorphogenesis. Moreover, the *Hoxa5* mutation affects the embryonic expression of epithelial regulators of lung development and function, such as the *Nkx2.1*, *Foxa2*, and *N-myc* genes. Its absence also causes a decrease in surfactant protein production in newborns. *Hoxa5* is still strongly expressed in postnatal lung, and surviving *Hoxa5*$^{-/-}$ adults present lung anomalies with deficient alveolar septation and atelectasis.[28,29] These anatomical limitations impact on the breathing pattern of *Hoxa5*$^{-/-}$ mice that compensate for their decreased alveolar surface area available for gas exchange by an increase in breathing frequency and overall minute ventilation. In humans, aberrant *HOXA5* expression has been shown to correlate with lung diseases.[30] Altogether, these data unambiguously establish a critical role for *Hoxa5* in lung ontogeny and point toward its implication in lung maturation and function. Here, we address the postnatal pulmonary function of the *Hoxa5* gene, with the objective of deciphering the etiology of the impaired postnatal lung development in *Hoxa5*$^{-/-}$ mice.

Materials and Methods

Mouse Strains and Genotyping

The establishment of the *Hoxa5* mutant mouse line in the MF1-129/SvEv-C57BL/6 mixed background has been previously described.[29] Embryonic age was estimated by considering the morning of the day of the vaginal plug as E0.5. Animals were genotyped by Southern blot analysis. *Hoxa5* mutant mice were intercrossed with *Pdgfα*$r^{GFP/+}$ mice (provided by Dr. Philippe Soriano, Fred Hutchinson Research Center, Seattle, WA). This mouse line carries a *green fluorescent* protein (*GFP*) allele fused to a *histone 2B* (*H2B*) moiety introduced into the *Pdgfαr* endogenous locus. The H2B portion allows the nuclear localization of GFP when expressed. The genotype of the *Pdgfα*r^{GFP} allele was determined by polymerase chain reaction.[31]

Tissue Collection and Histology

Wild-type and *Hoxa5*$^{-/-}$ mice were sacrificed at birth (P0), P5, P15, P31, and P60 (four wild-type and six mutant mice for each age). The body and wet lung weights were obtained by direct measurements for each specimen to determine the lung weight over the body weight ratio. Excised lungs were fixed overnight in ice-cold 4% paraformaldehyde prepared in phosphate-buffered saline. For P31 and P60 mice, lungs were fixed by tracheal instillation of ice-cold fixative until fully inflated under direct observation. Samples were processed, paraffin-embedded, and sectioned (4 μm) before staining according to standard procedures: hematoxylin and eosin (H&E) for alveolar morphology, periodic acid/Schiff for detection of mucus-producing goblet cells, Masson's trichrome for detection of ciliated cells, and Weigert to visualize elastic fibers. All experiments were performed according to the guidelines of the Canadian Council on

Animal Care and approved by the institutional animal care committee.

For GFP analysis of *Hoxa5;Pdgfαr*^{GFP} compound mutants, lungs from E16.5 embryos were harvested and fixed for 2 hours in ice-cold 4% paraformaldehyde. Samples were transferred in 30% sucrose and 0.2 mol/L phosphate buffer (40 mmol/L NaH_2PO_4, 150 mmol/L Na_2HPO_4) overnight at 4°C and then embedded in OCT. Cryostat sections (4 μm) were placed on poly-L-lysine-coated slides, counterstained with 10 μg/ml 4′6′-diamidino-2′-phenylindole (DAPI), and washed in phosphate-buffered saline (PBS) before mounting in aqueous media. For RNA preparation, lungs were snap-frozen in liquid nitrogen.

Proliferation, Apoptosis, and Immunohistochemical Analyses

To assess the proliferation rate, lung sections were immunostained with a rabbit polyclonal antibody against the phosphorylated histone H3 (pH3, 1/200 dilution; Upstate Biotechnology, Lake Placid, NY).[32] Apoptotic cells were detected by terminal transferase (TdT) DNA end labeling.[33] Cell types were revealed with the following antibodies: Clara cells with a goat polyclonal antibody reacting with rodent Clara cell secretory protein 10 (CC10, 1/400 dilution; provided by Dr. Gurmukh Singh, Veteran's Affairs Medical Center, Pittsburgh, PA); type II pneumocytes with a rabbit polyclonal antibody against SP-B (1/1000 dilution; Chemicon International, Temecula, CA), and a goat polyclonal antibody against Foxa2 (1/500 dilution, Santa Cruz Biotechnology, Santa Cruz, CA); alveolar myofibroblasts with a mouse monoclonal anti-α-smooth-muscle actin (α-SMA) antibody (1/10,000 dilution; Sigma Chemical Co., St. Louis, MO); and alveolar macrophages with a mouse monoclonal Mac-3 antibody (1/1000 dilution; Cedarlane, Hornby, ON, Canada). A chicken polyclonal antibody recognizing the mucin MUC5AC was obtained from Dr. Samuel Ho (1/15,000 dilution; University of Minnesota, Minneapolis, MN). A goat polyclonal antibody against mouse MMP-12 was also used (1/200 dilution; Santa Cruz). For Foxa2 immunostaining, ratio of positively stained cells on the total cell number was evaluated at P31 for a minimum of nine random areas with a total of at least 900 cells per specimen on average.

Bronchoalveolar Lavages, Cytokine, and MMP Activity Measurements

Bronchoalveolar lavages were performed on 3-month-old wild-type ($n = 23$) and *Hoxa5*$^{-/-}$ ($n = 19$) mice. For each animal, trachea was cannulated, and three 1-ml aliquots of saline were flushed into the lungs, withdrawn by syringe, pooled, and centrifuged.[34] Differential cell counts (a minimum of 100 cells/specimen) of bronchoalveolar lavage fluids (BALF) were performed on cytospin preparations after staining with Diff-Quik (Dade Diagnostics, Newark, DE). The levels of tumor necrosis factor (TNF)-α and interleukin (IL)-6 were measured in BALF of wild-type ($n = 18$) and *Hoxa5*$^{-/-}$ ($n = 15$) animals by enzyme-linked immunosorbent assay according to the manufacturer's directions (R&D Systems, Minneapolis, MN).

MMP activity was measured in macrophage-conditioned media isolated from adult wild-type and *Hoxa5*$^{-/-}$ mice ($n = 5$ per genotype) according to Wert and colleagues[35] with the following modifications. After a 24-hour culture of the macrophages isolated from BALF, the conditioned media were harvested, centrifuged (100,000 × *g*, 1 hour), and concentrated using Amicon Ultra-4 filtration devices (Millipore, Bedford, MA). The concentrated samples were then electrophoresed under non-reducing conditions into a 10% zymogram gelatin gel. A 30-μl aliquot of conditioned medium from HT1080 cells containing MMP2 and MMP9 activities was run in parallel.[36] Control gels were incubated in the presence of 20 mmol/L ethylenediaminetetraacetic acid before staining. These experiments were repeated three times, and Figure 7D is representative of the results obtained.

Tropoelastin Expression Analyses

Total RNA was isolated from P0, P5, P15, P31, P60, and adults (>4 months old) wild-type and *Hoxa5*$^{-/-}$ lungs (four wild-type and six mutant mice for each age) according to the TRIzol extraction protocol (Invitrogen, Carlsbad, CA). Northern blot analyses were performed using ^{32}P-labeled cDNA tropoelastin (provided by Dr. Elaine Davis, McGill University, Montréal, QC, Canada) and GAPDH probes to evaluate and compare elastin production. Northern blots were quantified with the NIH ImageJ software (Bethesda, MD).

Wounding and Boyden Chamber Assays of Primary Embryonic Lung Mesenchymal Cells

Lungs from E15.5 embryos, obtained by timed matings of *Hoxa5*$^{+/+}$ or *Hoxa5*$^{-/-}$ dams with *Hoxa5*$^{+/-}$;*Pdgfαr*$^{GFP/+}$ males, were dissected and dissociated by trypsin digestion to obtain single cell suspensions (five *Hoxa5*$^{+/+}$;*Pdgfαr*$^{GFP/+}$, four *Hoxa5*$^{+/+}$;*Pdgfαr*$^{+/+}$, 16 *Hoxa5*$^{-/-}$;*Pdgfαr*$^{GFP/+}$, and four *Hoxa5*$^{-/-}$;*Pdgfαr*$^{+/+}$ specimens). Mesenchymal cells were separated from epithelial cells by differential adhesion[37] and grown in Dulbecco's modified Eagle's medium containing 10% fetal bovine serum and penicillin/streptomycin until they reached confluency. Under these culture conditions, cells fully differentiated into smooth muscle cells.[37,38] Cultures were then starved by replacing the medium with Dulbecco's modified Eagle's medium containing 0.5% fetal bovine serum for 36 hours before wounding assays. These were performed by applying a sharp razor blade to monolayer cultures.[39] Plates were rinsed and low-serum medium was added. Invasion of the wounded area was followed under an inverted fluorescent microscope and pictures were taken at times 0, 12, and 24 hours after wounding. For Boyden chamber assays, primary E15.5 lung mesenchymal cells (six *Hoxa5*$^{+/+}$;*Pdgfαr*$^{GFP/+}$, three *Hoxa5*$^{+/+}$;

Pdgfαr$^{+/+}$, eight *Hoxa5*$^{-/-}$;*Pdgfαr*$^{GFP/+}$, and four *Hoxa5*$^{-/-}$;*Pdgfαr*$^{+/+}$ specimens) were cultured as described above. Once confluent, cells were starved for 24 hours and then trypsinized and counted.[40] A total of 1×10^5 cells were added to the upper compartment of Boyden chambers (8.0-μm pore size; Falcon; BD Biosciences Discovery Labware, Bedford, MA) that were previously coated with 0.1% gelatin. Each specimen was analyzed in triplicates. Cells were allowed to migrate for 24 hours in low-serum medium. Non-migratory cells were removed from the upper membrane surface with a cotton swab. The migratory cells were then fixed in 95% ethanol and 5% acetic acid for 10 minutes followed by Harris's hematoxylin staining overnight. After several water washes, cells from five fields per triplicate were counted.

In parallel, primary lung mesenchymal cultures were tested for wounding assays with a 1000-μl pipette tip. After either the razor blade or the Boyden chamber assays, some cultures were subsequently plated in 10% fetal bovine serum-containing medium until they reached confluency (two *Hoxa5*$^{+/+}$;*Pdgfαr*$^{GFP/+}$, nine *Hoxa5*$^{+/+}$;*Pdgfαr*$^{+/+}$, 15 *Hoxa5*$^{-/-}$;*Pdgfαr*$^{GFP/+}$, and 13 *Hoxa5*$^{-/-}$;*Pdgfαr*$^{+/+}$ specimens). They were then starved for 48 hours before wounding with a 1000-μl pipette tip.[41] After the scratch, plates were rinsed and low-serum medium was added. Pictures were taken at times 0, 12, and 24 hours to follow the invasion of the wounded area by the cells.

Immunofluorescence Analysis

Primary E15.5 lung mesenchymal cells were trypsinized and plated on poly-L-lysine-coated coverslips and cultured overnight in Dulbecco's modified Eagle's medium supplemented with 10% fetal bovine serum. Cells were fixed with 2% paraformaldehyde in PBS for 10 minutes, followed by one wash in PBS and 0.1% Triton and two washes in PBS. After a 10-minute incubation with blocking solution (PBS with 2% bovine serum albumin and 0.5% normal goat serum), cells were incubated with primary antibodies for 3 hours at room temperature. The Hoxa5 rabbit polyclonal and the α-smooth muscle actin mouse monoclonal antibodies were used at a dilution of 1/200[42] and 1/1000, respectively. After three washes, cells were incubated with the appropriate Alexa Fluor 594 and Alexa Fluor 488 secondary antibodies and 10 μg/ml DAPI for 1 hour at room temperature. For some specimens, phalloidin-rhodamine (1/200) was added. Cells were washed and mounted in aqueous medium.

Statistical Analysis

Repeated measures for the linear mixed model were performed to assess the difference between genotypes at all stages studied when genotype is considered the fixed effect and area is the random effect. The procedure PROC MIXED from the SAS System (Cary, NC) was used.[43] A Student's *t*-test was performed for Foxa2 immunostaining positivity and for Boyden chamber assays.

Results

Abnormal Lung Morphology in Hoxa5$^{-/-}$ *Mice*

Embryonic lung development is perturbed in *Hoxa5*$^{-/-}$ mutants leading to a high rate of perinatal lethality.[27] Surviving adult mutants present a severe emphysema-like phenotype characterized by enlarged airspaces and an overall decrease in septa number.[28] On macroscopic examination, some areas of *Hoxa5*$^{-/-}$ lungs were completely depleted of alveoli, whereas others showed large tubular structures (shown for P31; Figure 1, K and L). To assess the origin of the morphological defects, lung histological analyses were performed at different ages after birth. At P0, wild-type lungs showed expanded respiratory saccules (Figure 1A). In contrast, *Hoxa5*$^{-/-}$ lungs were collapsed with a thickened parenchymal layer, consistent with the tragic outcome that accompanies the loss of *Hoxa5* function (Figure 1B).[27] At P5, growing septa were observed in wild-type lungs, whereas very few were seen in *Hoxa5*$^{-/-}$ specimens (Figure 1, C and D). At P15, only some alveoli were formed in *Hoxa5*$^{-/-}$ samples and airspace enlargement was already obvious compared with wild-type lungs (Figure 1, E and F). These alterations became more prominent with age (Figure 1, G–J). Areas of atelectasis were also detected (Figure 1H). These results suggest that the emphysema-like morphology observed in *Hoxa5*$^{-/-}$ animals originated from impaired septation, a key process in pulmonary alveogenesis. They also support the notion that *Hoxa5* plays a critical role in postnatal lung development.

Consequences of the Hoxa5 Mutation on Pulmonary Weight, Proliferation, and Apoptosis

To explore the etiology of the septation defect, we first analyzed lung growth by measuring the lung weight/body weight ratio at different ages (Figure 2A). No significant difference was observed between the body weight of wild-type and *Hoxa5*$^{-/-}$ mice from P0 to adult age. At P0, P5, and P15, the ratio was statistically lower for *Hoxa5*$^{-/-}$ animals ($P < 0.0075$). However, the difference was resolved by P31 suggesting that recovery occurred.

To decipher the underlying cellular process involved in the lung growth discrepancy, we examined lung proliferation and apoptosis. Compared with wild-type samples, decreased proliferation was first observed in P0 and P5 *Hoxa5*$^{-/-}$ lungs (Figure 2, B, C, and H). This was followed by increased proliferation at P15 and P31 (Figure 2, D–H). This increase could not be associated to a specific cell type. No significant difference was noted at P60 (Figure 2H). The changes in the temporal profile of proliferation in *Hoxa5*$^{-/-}$ lungs could explain the lower lung weight/body weight ratios observed at early stages and the compensatory effect seen later on.

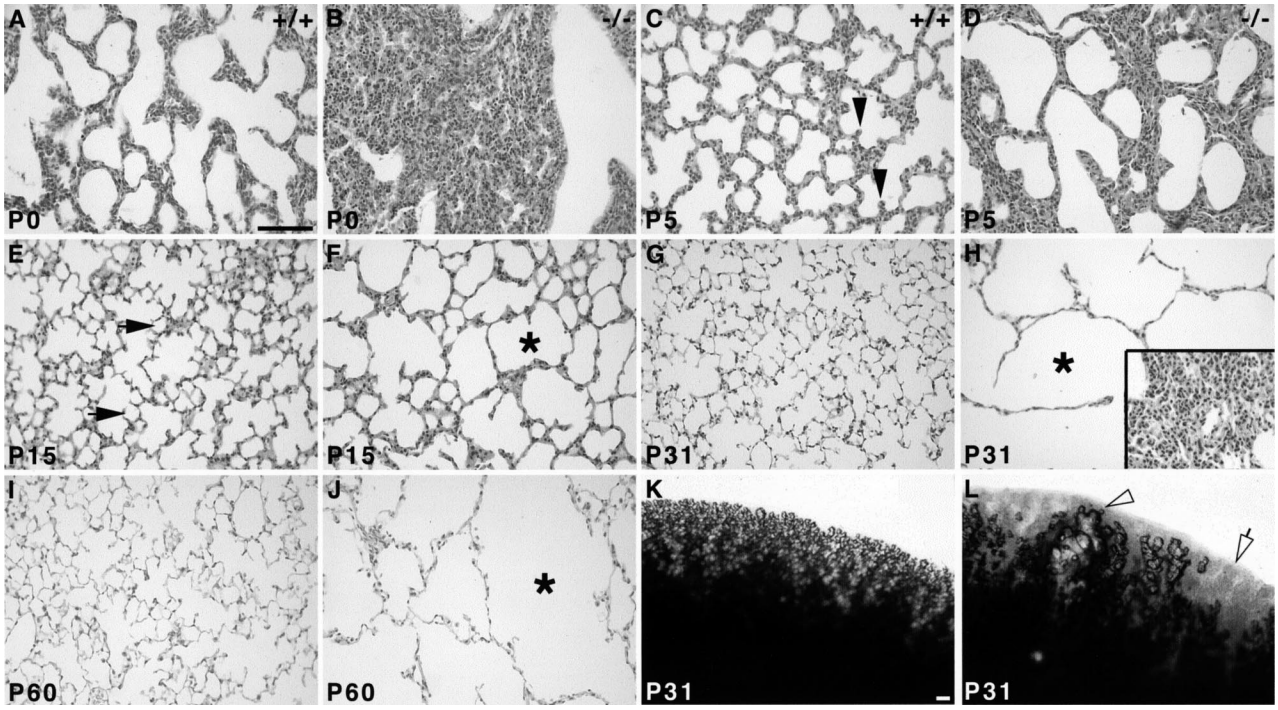

Figure 1. Comparative histology (**A–J**) and macroscopic analysis (**K**, **L**) of postnatal wild-type and *Hoxa5*$^{-/-}$ lungs. At P0, mutant lungs were collapsed in contrast to wild-type specimens (**A**, **B**). Alveogenesis initiated normally at P5 in control samples (**C**, **arrowheads**), whereas in *Hoxa5*$^{-/-}$ lungs, the parenchyma was thickened and few septa were noticed (**D**). At P15, alveoli were readily observed in controls (**E**, **arrows**), but *Hoxa5*$^{-/-}$ lungs rather displayed enlarged airspaces (**F**, **asterisk**). At P31 (**G**, **H**, **K**, **L**) and P60 (**I**, **J**), *Hoxa5*$^{-/-}$ lungs presented an emphysema-like phenotype (**H**, **J**, **L**) with areas depleted of alveoli (**open arrow** and **asterisk**) or large tubular structures (**open arrowhead**), whereas other regions were atelectatic (**inset** in **H**) when compared with the normal lung architecture (**G**, **I**, **K**). Scale bars = 100 μm.

We also investigated the contribution of apoptosis to the phenotype. Consistent with the low apoptotic rate normally observed in postnatal lungs,[44] few positive cells were detected by terminal dUTP nick-end labeling (TUNEL) assay in the pulmonary tissue of both wild-type and *Hoxa5*$^{-/-}$ specimens at all stages tested (not shown). Thus, apoptosis did not contribute significantly to the delayed lung growth. These findings showed that the absence of *Hoxa5* function impacts on lung proliferation during the critical period of alveogenesis without altering programmed cell death.

Altered Cell Specification in Hoxa5$^{-/-}$ *Respiratory Tract*

The mature respiratory tract epithelium is lined by a variety of cell types accomplishing specialized functions that guarantee proper lung homeostasis. The fact that surfactant protein production is reduced at birth in *Hoxa5*$^{-/-}$ pups,[27] combined with our observations that the *Hoxa5* mutation perturbs epithelial cell specification in the stomach[32] prompted us to determine whether changes in cell specification occurred in the lung epithelium as well. Using SP-B as a marker, we examined type II pneumocytes, an epithelial cell type that maintains fluid homeostasis in the alveolar lumen and secretes surfactant. From P5 onwards, the number and the localization of SP-B-positive cells in the alveolar parenchyma were not altered in *Hoxa5*$^{-/-}$ lungs compared with wild-type samples (shown for P60; Figure 3, A and B). However, a secreted proteinaceous material reacting with the antibody was detected in the collapsed lungs of P0 mutants (not shown). Foxa2 immunostaining confirmed the normal distribution of type II pneumocytes in the distal lung but also revealed a small but significant increase in their number in P31 *Hoxa5*$^{-/-}$ lungs (22.25 ± 3.26% Foxa2-positive cells in wild-type versus 25.32 ± 4.91% in *Hoxa5*$^{-/-}$ specimens; $P < 0.0002$; not shown). This likely reflected the increased proliferation observed at this age (Figure 2H). Thus, the decreased surfactant protein production occurring in *Hoxa5*$^{-/-}$ newborns does not result from a change in cellularity but rather from reduced surfactant protein gene expression as already shown.[27]

Using a CC10-specific antibody, we also looked at Clara cells, a nonciliated secretory cell type normally localized along the bronchial tree and bronchioles. Clara cells were similarly detected along the respiratory bronchi and bronchioles for both genotypes from birth to P60 (Figure 3, C and D). The ciliated columnar cells and the mucus-secreting goblet cells are the major cell types lining the proximal respiratory epithelium, and they constitute the primary barrier against pathogenic agents. No major difference was noted for ciliated cells between wild-type and mutant specimens from birth to adulthood (Figure 3, E and F). However, we noticed a higher proportion of goblet cells in the epithelium of the trachea and the bronchi of *Hoxa5*$^{-/-}$

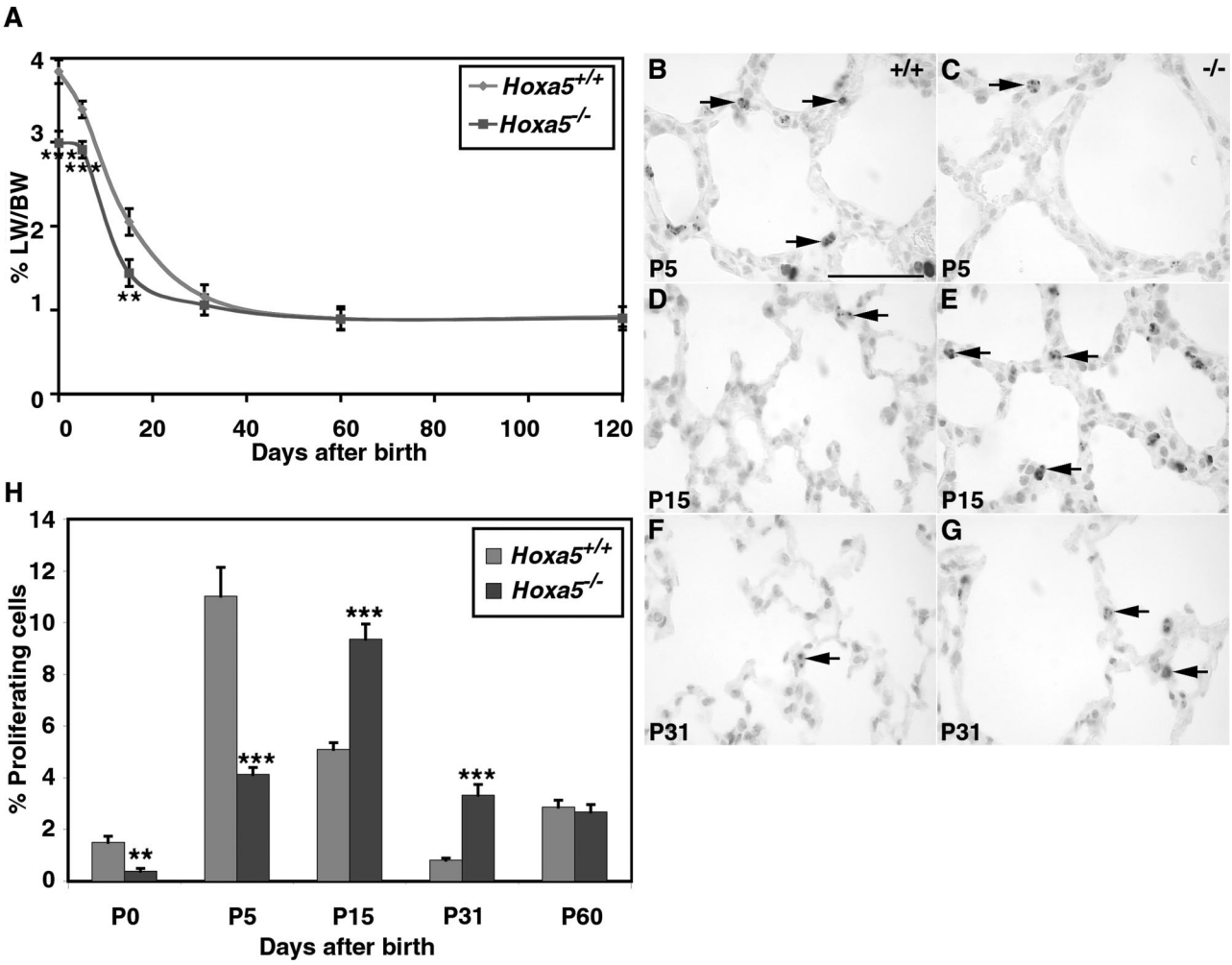

Figure 2. Lung weight/body weight ratio (**A**) and proliferation rate (**B–H**) of wild-type and *Hoxa5*$^{-/-}$ lungs. **A:** The lung weight/body weight (LW/BW) ratio of *Hoxa5*$^{-/-}$ mutants was statistically lower than that of controls at P0, P5, and P15. However, a compensatory effect was observed from P31 onwards. Detection of proliferating cells with an anti-phosphorylated histone H3 antibody (**B–G**, **arrows**) showed that proliferation was lower in *Hoxa5*$^{-/-}$ specimens compared with wild-type lungs at P0 (**H**) and P5 (**B**, **C**, **H**). At P15 (**D**, **E**, **H**) and P31 (**F–H**), more proliferating cells were detected in mutant lungs than in controls. **H:** No difference was observed at P60 between both groups. Statistically significant differences are denoted by **asterisks** (**$P < 0.0075$, ***$P < 0.0006$). Scale bar = 50 μm.

mutants, which prompted us to further examine this cell population. Although goblet cells were only sparsely found in the trachea and primary bronchi of wild-type specimens, they were dramatically increased along the trachea and the primary bronchi of mutant samples (Figure 4). Furthermore, they ectopically arose in more distal structures such as the secondary bronchi and bronchioles (Figure 4, B, D, F, H, and J). This augmentation in goblet cell number was already detected at E18.5 (not shown). From P15 onwards, the severity of the hyperplasia was salient (Figure 4, E–J). In experimentally induced mucus hypersecretion of the respiratory airways, *Muc5ac* gene expression is observed.[45] When *Hoxa5*$^{-/-}$ samples were immunostained with the MUC5AC antibody, positive cells were readily visualized along the bronchi of the mutant lungs from P15 onwards, whereas control tissues remained negative (shown for P31; Figure 4, K and L). Thus, the loss of *Hoxa5* function affects the specification of goblet cells and causes hyperplasia, metaplasia, and mucus hypersecretion.

Anomalies in Alveolar Myofibroblasts Localization and in Elastin Deposition in Hoxa5$^{-/-}$ *Lungs*

We also looked at alveolar myofibroblasts because they are a prominent player in alveoli formation. These cells are normally localized at the tip of growing septa where they synthesize and deposit elastic fibers.[7] Elastogenesis is a highly regulated process that first peaks at birth and then at P10 to P14. Afterward, it declines through maturation to reach unappreciable levels in the adult mouse lung.[46] The α-SMA marker was used to reveal alveolar myofibroblasts. As expected, these cells were found at the tip of the growing septa in wild-type specimens at P5 and P15 (Figure 5, A and C). However in *Hoxa5*$^{-/-}$ lungs,

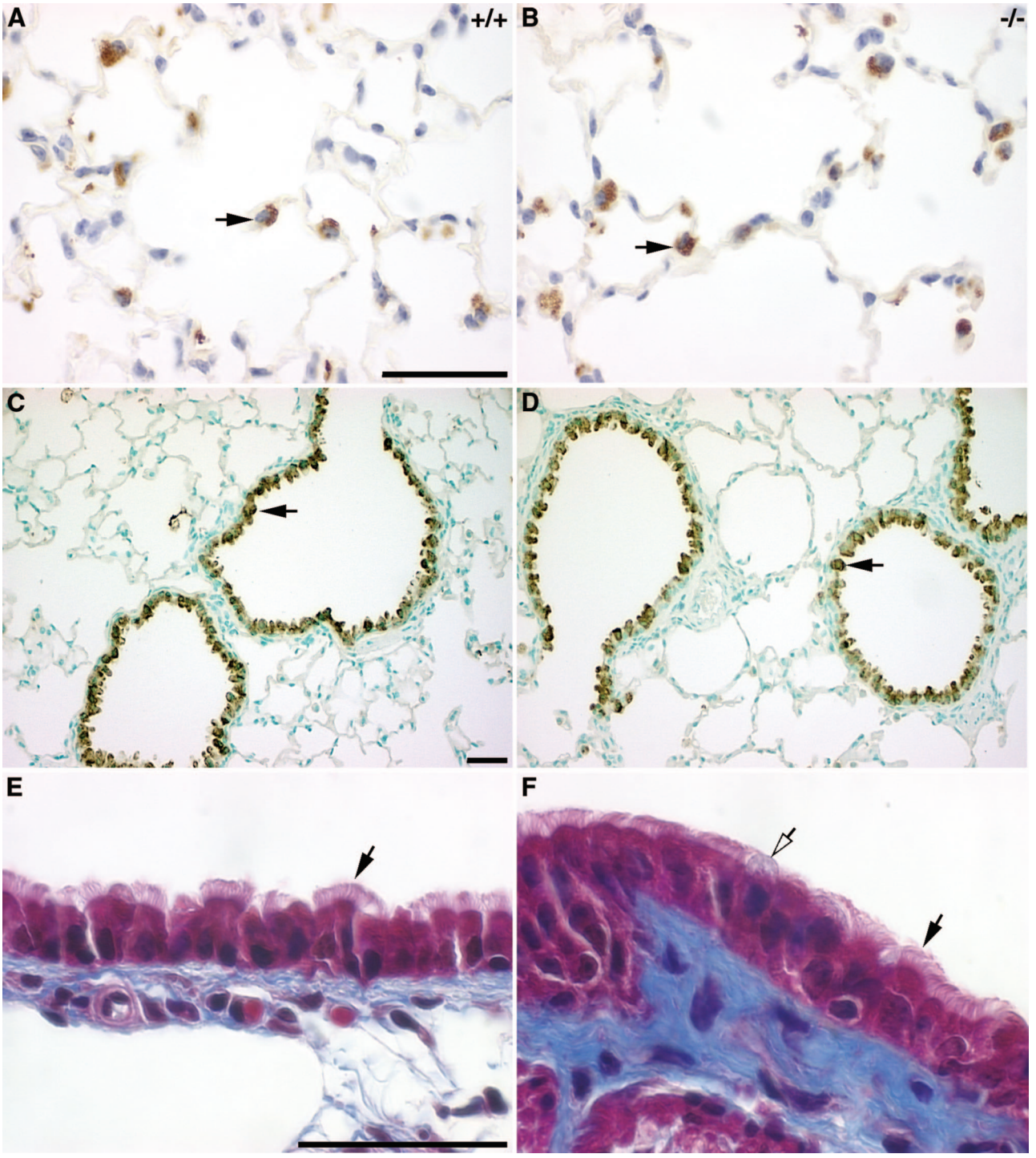

Figure 3. Correct specification of type II pneumocytes (**A**, **B**), Clara cells (**C**, **D**), and ciliated cells (**E**, **F**) in *Hoxa5*$^{-/-}$ lungs. No major difference was detectable between wild-type and *Hoxa5*$^{-/-}$ lungs regarding type II pneumocytes and Clara cells as shown by immunostaining with SP-B (**A**, **B**) and CC-10 (**C**, **D**) antibodies specific for these cell types, respectively (**black arrows**, shown for P60). Masson's trichrome revealed that ciliated cells (**black arrows**) were similarly distributed in mutant (**E**) and wild-type lungs (**F**). However, mucus-producing goblet cells were more often visualized in mutant samples (**F**, **open arrow**). Scale bars = 50 μm.

alveolar myofibroblasts appeared trapped in the parenchyma surrounding alveoli (Figure 5, B and D). Later on, α-SMA expression decreased in alveolar myofibroblasts rendering their presence undetectable for both genotypes (not shown).[47]

To determine whether the abnormal distribution of alveolar myofibroblasts observed in mutants correlated with anomalies in elastin deposition, Weigert staining was performed (Figure 5, E–L). Before birth, elastic fiber formation appeared normal in both groups (not shown). In

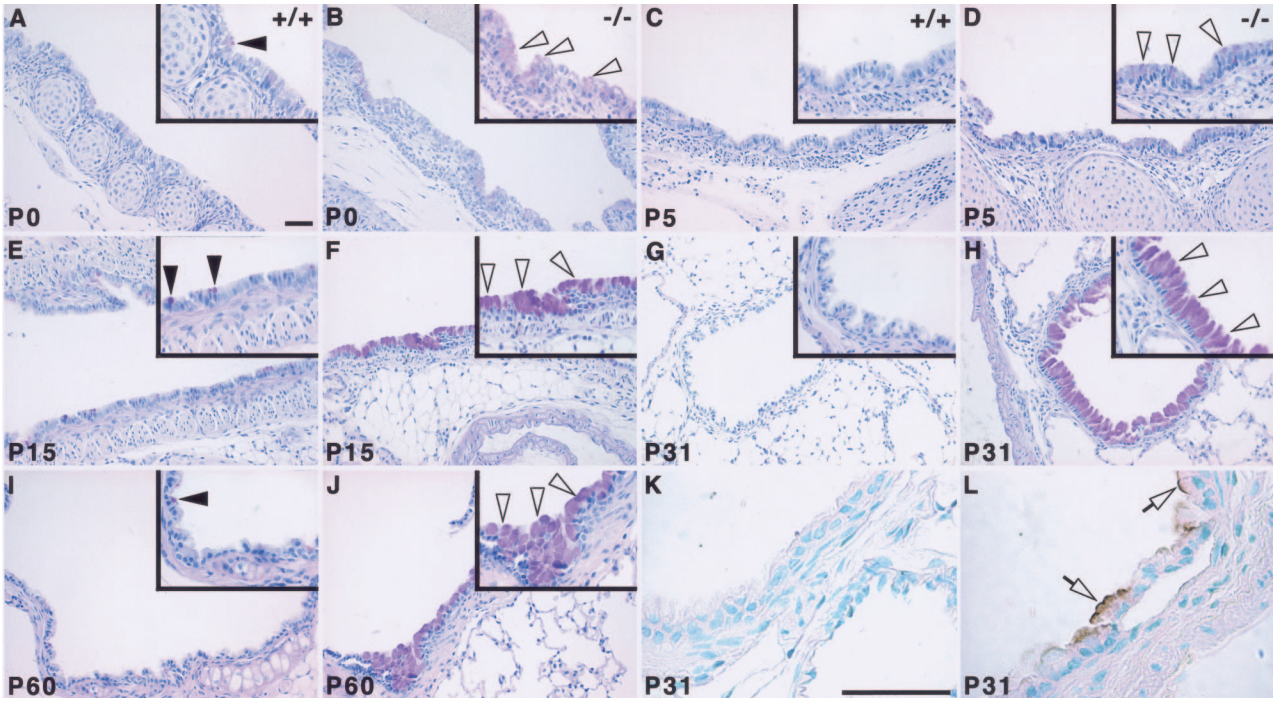

Figure 4. Goblet cell abnormal distribution in *Hoxa5*$^{-/-}$ lungs. Goblet cells were revealed by periodic acid/Schiff staining in postnatal lungs (**A–J**). At all ages tested, only a few positive cells were detected in wild-type samples (**A**, **C**, **E**, **G**, **I**; **arrowheads**), mostly scattered along the epithelium of the trachea (**A**, **C**) and the primary bronchi (**E**, **I**). No goblet cell was detected distally to the primary bronchi in controls (**G**). In *Hoxa5*$^{-/-}$ lungs, an increase in goblet cell number was systematically observed at every stage (**B**, **D**, **F**, **H**, **J**; **open arrowheads**), most obviously from P15 onwards (**F**, **H**, **J**). Furthermore, positive cells were detected in more distal structures such as the secondary bronchi (**H**) and bronchioles (not shown). Mucin MUC5AC, a marker of mucus hypersecretion, was detected by immunostaining (**K**, **L**). Although control samples remained negative (**K**), positive cells stained at their apical side were observed along the bronchi of *Hoxa5*$^{-/-}$ specimens from P15 onwards (shown for P31; **L**, **open arrows**). Scale bars = 50 μm.

P0 and P5 controls, elastin was deposited at the tip of the septa and along the respiratory saccules, as expected (Figure 5, E and G).[8] In contrast, elastic fibers were disorganized and aberrantly distributed within the pulmonary tissue of P0 and P5 *Hoxa5*$^{-/-}$ lungs (Figure 5, F and H). From P15 onwards, the fibers appeared more abundant, disorganized, and fragmented (Figure 5, I–L). Northern analyses of tropoelastin expression failed to reveal differences in tropoelastin transcript levels between wild-type and *Hoxa5*$^{-/-}$ lungs at all ages examined that would correlate with the elastic fiber anomalies seen in mutants (not shown). Thus, *Hoxa5* function is required for the correct positioning of alveolar myofibroblasts, which in turn warrants proper elastin deposition and septa formation, both being essential for normal lung architecture and function.

Inflammatory Response in Hoxa5$^{-/-}$ *Lungs*

Goblet cell hyperplasia and mucus hypersecretion can be associated to the recruitment of inflammatory cells in the lung.[4] Because inflammatory cells were detected in P60 *Hoxa5*$^{-/-}$ specimens (Figure 5L), we tested for the putative involvement of inflammation in *Hoxa5*$^{-/-}$ postnatal lung phenotype. Although immunostaining with a Mac-3 macrophage marker detected a few sparse positive cells in controls, a high percentage of macrophages was observed in mutant lungs (Figure 6, A–C). This increase was statistically significant from birth to adulthood, except for P15. Macrophages from *Hoxa5*$^{-/-}$ lungs also presented an atypical morphology indicative of an inflammatory response.

We performed bronchoalveolar lavages to further assess the importance of this inflammatory response in *Hoxa5*$^{-/-}$ lungs. Microscopic observations of recovered cells confirmed the hypertrophic and foamy morphology of the macrophages in mutant samples (Figure 7, B and C). Moreover, *Hoxa5*$^{-/-}$ BALF cell count was higher than that of controls and a statistically significant increase was observed for each inflammatory cell type identified (Figure 7A). Vacuolated macrophages constituted the predominant cell population in mutant specimens. These data confirmed that *Hoxa5*$^{-/-}$ lungs were under an inflammatory challenge.

Resident macrophages and recruited monocytes play a major role in amplifying the inflammatory response in the lower respiratory tract through the increased production of proinflammatory cytokines, such as TNF-α and IL-6.[48] TNF-α is also a main participant in the activation of macrophages to produce MMPs involved in lung remodeling. The levels of TNF-α and IL-6 were measured by enzyme-linked immunosorbent assay assays in BALF. No statistically significant difference in cytokine levels was detected between both genotypes (not shown). Considering the augmentation in macrophages and the abnormal aspect of elastic fibers in *Hoxa5*$^{-/-}$ lungs, we immunostained lung sections with a specific antibody against MMP-12, a major elastolytic protease produced by activated alveolar macrophages.[49] The majority of macrophages stained positively for MMP-12 in mutant samples,

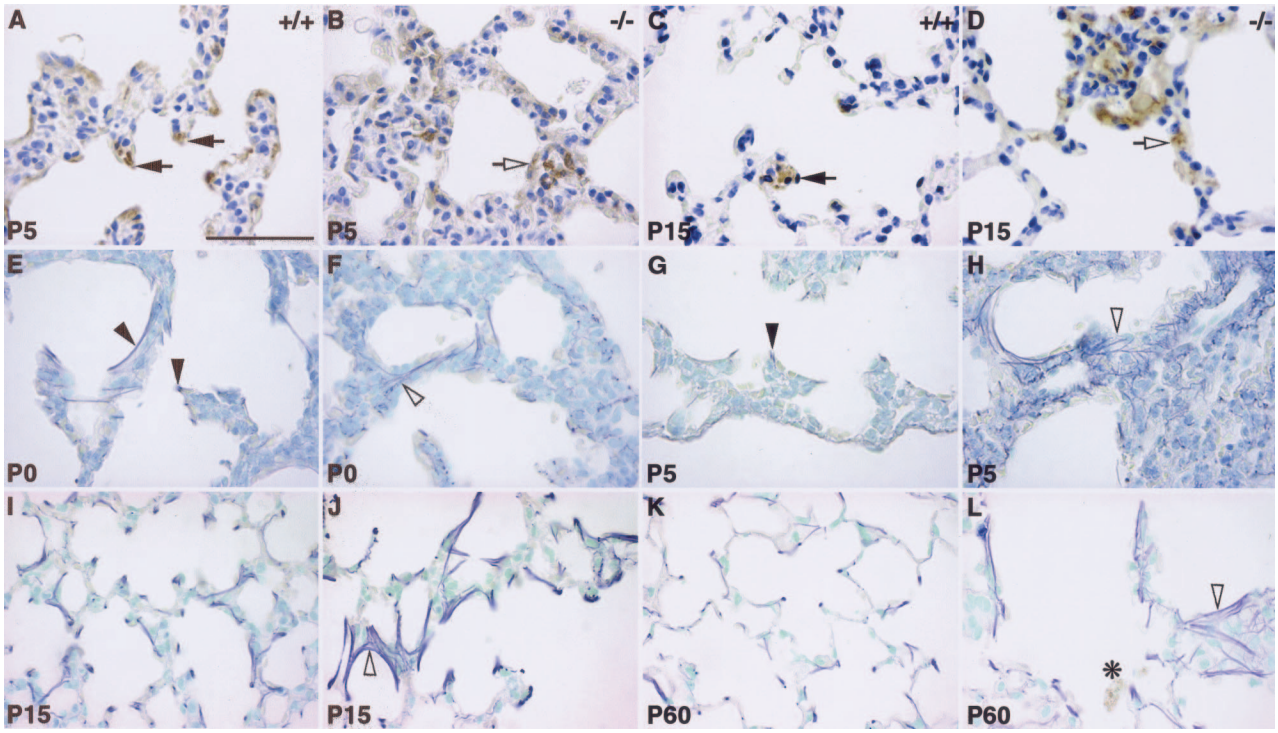

Figure 5. Perturbed alveolar myofibroblasts localization (**A–D**) and elastin deposition (**E–L**) in *Hoxa5*$^{-/-}$ lungs. Alveolar myofibroblasts were located at the tip of the septa of control specimens at P5 and P15, as revealed by immunostaining with an α-SMA antibody (**A**, **C**; **arrows**). In *Hoxa5*$^{-/-}$ lungs, they were trapped within the parenchyma (**B**, **D**; open **arrow**). Weigert staining allowed visualization of elastic fibers (**E–L**). In P0 and P5 control specimens, elastic fibers were localized along the respiratory saccules and at the tip of the growing septa (**E**, **G**; **arrowheads**). In *Hoxa5*$^{-/-}$ lungs, elastin appeared tangled in the parenchyma (**F**, **H**; **open arrowhead**). At P15 onwards, *Hoxa5*$^{-/-}$ lungs displayed disorganized fibers (**J**, **L**; **open arrowhead**) compared with wild-type lungs (**I**, **K**). Moreover, inflammatory cells were detected in P60 mutant lungs (**L**, **asterisk**). Scale bar = 50 μm.

suggesting enhanced elastase production in *Hoxa5*$^{-/-}$ lungs (shown for P60; Figure 6, D and E). The proteinase activity present in wild-type and *Hoxa5*$^{-/-}$ alveolar macrophage-conditioned media was also directly tested by zymogram assays on gelatin gels. In the representative experiment shown in Figure 7D, 5.8×10^4 and 27.9×10^4 cells were obtained from pools of five wild-type and five *Hoxa5*$^{-/-}$ animals, corresponding to 81 and 282 μg of proteins, respectively. Because of the augmented macrophage number, the *Hoxa5*$^{-/-}$-conditioned medium showed slightly elevated MMP9 and MMP2 activities (Figure 7D). Under these conditions, MMP12 activity was not detected. Thus, the absence of *Hoxa5* function leads to an inflammatory response associated with augmented MMP production and activities.

Impaired Dispersal of Alveolar Myofibroblast Progenitors in Hoxa5$^{-/-}$ *Lungs*

Pdgfαr-positive cells most likely constitute the progenitors of alveolar myofibroblasts responsible for elastin deposition.[11] We took advantage of the *Pdgfαr*$^{GFP/+}$ mouse line carrying a *GFP* knocked-in allele at the *Pdgfαr* locus to follow the progenitor population and its behavior in *Hoxa5*$^{-/-}$ lungs.[31] GFP staining faithfully reproduces the native wild-type *Pdgfαr* expression pattern in the *Pdgfαr*$^{GFP/+}$ mouse line and thus can serve as a lineage tracer. Before the canalicular stage and up until E15.5, clusters of *Pdgfαr*-positive cells occur at the distal epithelial branches. Between E16.5 and E17.5, these cells multiply and spread to acquire positions as solitary cells in the terminal sac walls. It was previously proposed that a prenatal block in the distal spreading of the alveolar myofibroblast precursors could result in alveolar septation failure.[11,13] When we assessed the distribution of *Pdgfαr/GFP*-expressing cells in E16.5 *Hoxa5*$^{+/+}$ lungs, they displayed the expected behavior being dispersed in the lung parenchyma (Figure 8A). In contrast, most *Pdgfαr/GPF*-positive cells remained clustered around the epithelium in *Hoxa5*$^{-/-}$ lungs, indicating a failure of the alveolar myofibroblast progenitors to distally spread (Figure 8B). Areas devoid of progenitors were also found, indicating their incapacity to reach certain regions of the lung (Figure 8C). These observations suggested that the *Hoxa5*$^{-/-}$ impaired alveogenesis may originate from the inability of alveolar myofibroblast progenitors to properly invade the developing lung.

To address if a cell motility problem could underlie the defective dispersal of alveolar myofibroblast progenitors, we performed wounding assays on primary mesenchymal cells isolated from lungs of E15.5 *Hoxa5*$^{+/+}$ and *Hoxa5*$^{-/-}$ embryos carrying or not the *Pdgfαr*^{GFP} allele. If the *Hoxa5* mutation affects the motility of alveolar myofibroblast precursors, *GFP*-expressing cells should be impaired in their capacity to invade the denuded area in wounding assays. Under the culture condition applied, mesenchymal pulmonary cells differentiated into smooth muscle cells as dem-

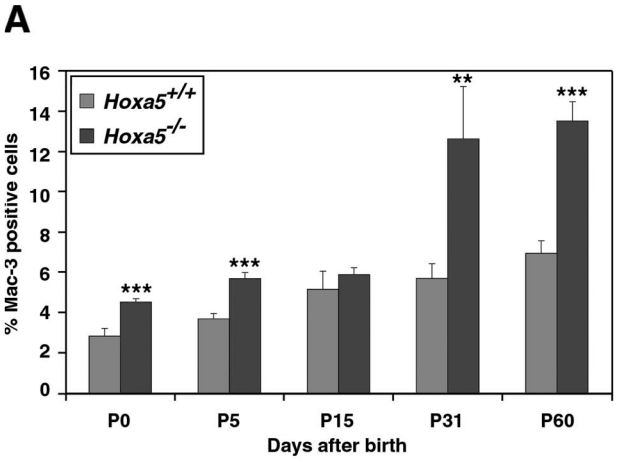

Figure 6. Increased percentage of alveolar macrophages in *Hoxa5*$^{-/-}$ lungs. A Mac-3-specific antibody was used to detect macrophages in the lung (**A–C**, **arrows**) showing that the proportion of macrophages was statistically higher in *Hoxa5*$^{-/-}$ lungs than in controls. **Asterisks** denote statistical differences (**$P <$ 0.01, ***$P < 0.005$). **C:** Moreover, at P31 (not shown) and P60, accumulation of large vacuolated macrophages was observed in *Hoxa5*$^{-/-}$ lungs. MMP-12 immunostaining revealed that the majority of macrophages in mutant samples produced this elastase (shown for P60; **D** and **E**, **open arrows**). Scale bar = 50 μm.

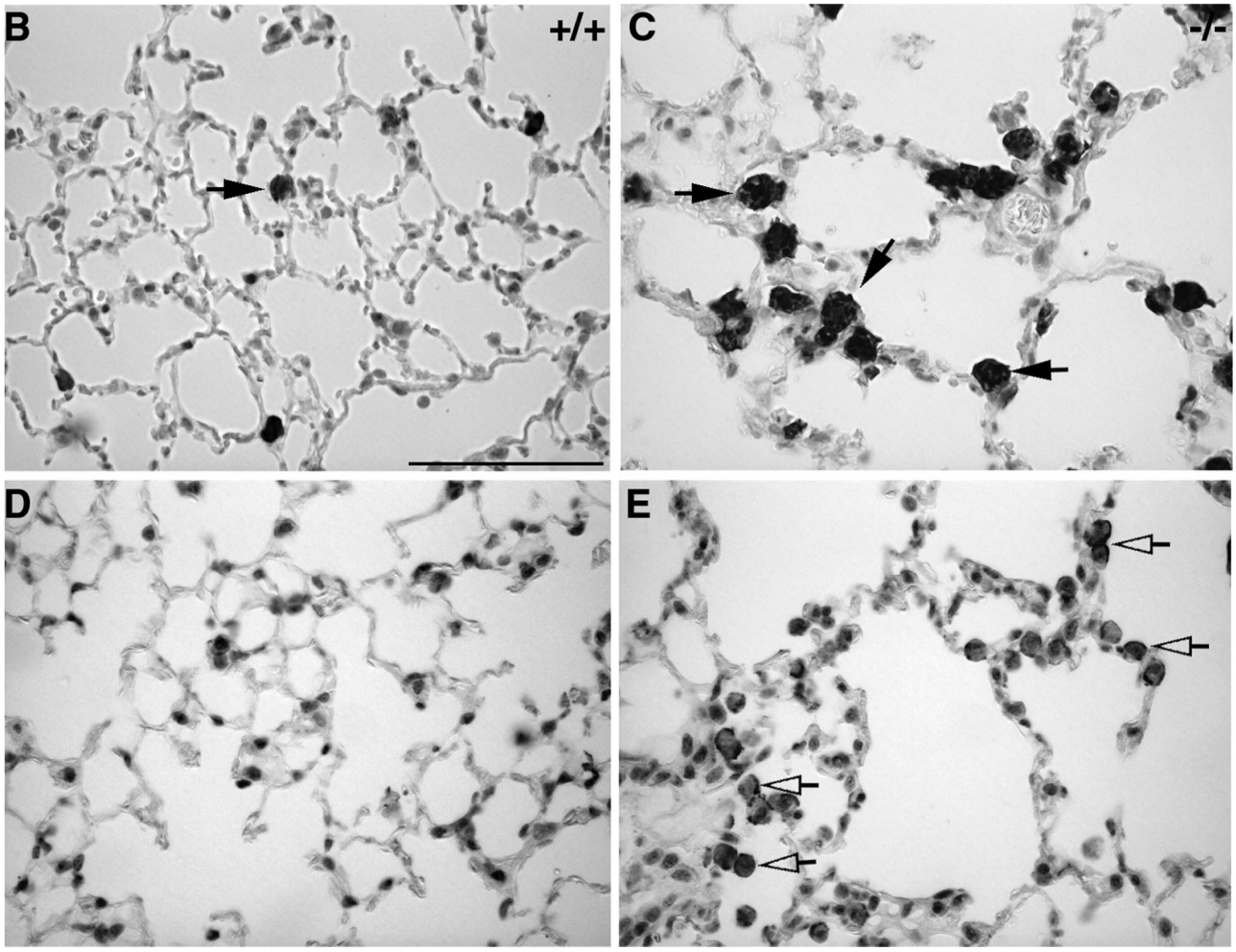

onstrated by the expression of α-SMA (Figure 9A) and that of GFP (Figure 8, E, G, I, K, M, and O; Figure 9, A and B).[37,38] In razor blade wounding assays, four of five *Hoxa5*$^{+/+}$*;Pdgfαr*$^{GFP/+}$ cultures displayed extensive invasion of the denuded area, whereas 11 of 16 *Hoxa5*$^{-/-}$*;Pdgfαr*$^{GFP/+}$ cultures showed a reduced capacity to do so. This difference in behavior was also confirmed by scratch assays with a pipette tip (Figure 8, D–O). Within 24 hours, 10 of 11 wild-type samples filled the scratch (Figure 8, H and I). In contrast, 17 of 28 *Hoxa5*$^{-/-}$ cultures were impaired in wound closure (Figure 8, N and O). Migration in Boyden chambers was also tested but no difference in the migratory behavior in response to gelatin could be revealed between both genotypes (wild type: 55.9 ± 22.9 cells, $n = 9$; *Hoxa5*$^{-/-}$: 61.0 ± 31.2 cells, $n = 12$; $P = 0.07$). Thus, these results established a role for *Hoxa5* in mesenchymal cell motility and indicated a mechanism

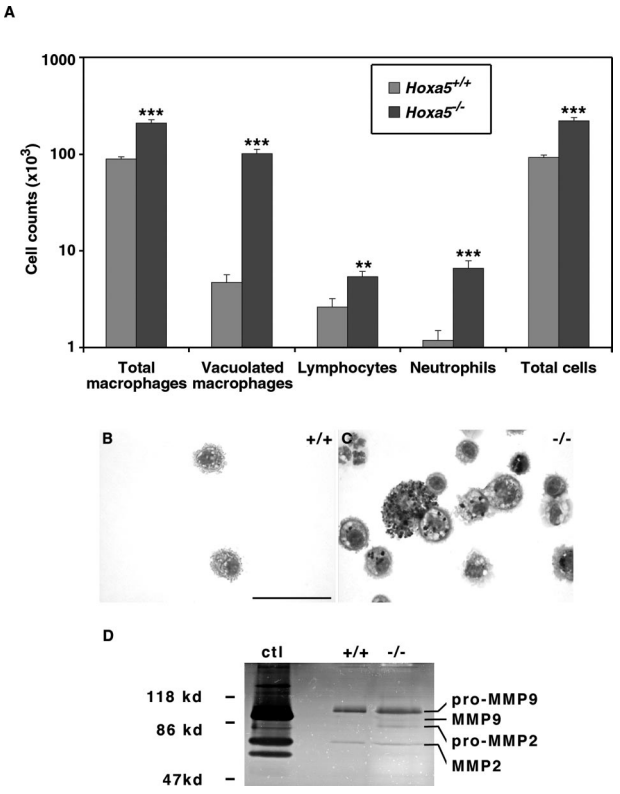

Figure 7. Increased number of inflammatory cells and MMP activity in *Hoxa5*$^{-/-}$ BALF. **A:** Differential cell counts showed an increase of macrophages, lymphocytes, and neutrophils in *Hoxa5*$^{-/-}$ specimens when compared with controls. Statistically significant differences are denoted by **asterisks** (**$P < 0.002$, ***$P < 0.0001$). Diff-Quik staining also revealed that *Hoxa5*$^{-/-}$ BALF contained large, vacuolated macrophages with dark inclusions not seen in control samples (**B**, **C**). **D:** MMP activities in wild-type (+/+) and *Hoxa5*$^{-/-}$ (−/−) alveolar macrophage-conditioned media in gelatin gel zymogram. Data are presented as the reverse image of the original zymogram. Conditioned media from the HT1080 cell line served as a positive control (ctl). Slightly elevated MMP2 and MMP9 activities were observed in *Hoxa5*$^{-/-}$ alveolar macrophage-conditioned medium. Scale bar = 50 μm.

by which the lack of *Hoxa5* function compromises the spreading of alveolar myofibroblast progenitors into the parenchyme during embryonic lung development.

Hoxa5 Expression in the Lung Mesenchyme

To assess whether *Hoxa5* exerts a cell-autonomous effect on alveolar myofibroblast cell specification, Hoxa5 immunofluorescence analyses were performed on primary embryonic lung mesenchymal cells. The Hoxa5 protein was detected in the nuclei of embryonic lung myofibroblasts (Figure 9C), in concordance with our previous observations that *Hoxa5* transcripts were restricted to the lung mesenchyme during embryonic development.[27] These myofibroblasts also produced α-SMA and the Pdgfα receptor as evidenced by the GFP labeling (Figure 9, A and B). Hoxa5 immunostaining in wild-type primary myofibroblasts substantially overlapped with Pdgfα receptor expression (Figure 9, D–G). As expected, Hoxa5 was not detected in *Hoxa5*$^{-/-}$ cells (Figure 9, H–K). No expression of *Hoxa5* was observed in the embryonic and postnatal lung epithelia, precluding a direct role of *Hoxa5* in goblet cell specification (not shown).[27] Thus, *Hoxa5* could regulate the specification and the behavior of alveolar myofibroblast progenitors in a cell-autonomous manner.

Discussion

Hoxa5 Carries a Broad Spectrum of Activities during Lung Development and Maturation

Hoxa5 function is instrumental throughout lung ontogeny and maturation. During embryogenesis, *Hoxa5* participates in the development of the respiratory tract where it exerts its action through the regulation of mesenchymal-epithelial interactions (J.A. and L.J., unpublished).[27] After birth, *Hoxa5* plays a prominent role in alveogenesis initiation and lung homeostasis because the *Hoxa5* mutation causes impaired septa formation, goblet cell hyperplasia, and accumulation of inflammatory cells. The involvement of *Hoxa5* in postnatal processes is also exemplified by its requirement for proper gut maturation and mammary gland development.[50,51] The panoply of postnatal phenotypes displayed by *Hox* mutants indicates that aside from the crucial role of *Hox* genes in embryo patterning, they fulfill a variety of functions in adult life.[19]

Our study indicates that the postnatal lung defects of *Hoxa5*$^{-/-}$ mutants have an embryonic origin, pointing to altered cell specification and behavior of goblet cells and alveolar myofibroblast progenitors. Because *Hoxa5* remains expressed in the adult lung,[29] a definitive approach to establish the *Hoxa5* postnatal role would be to conditionally ablate the gene function in the lung after birth.

Hoxa5 Impacts on Proliferation but Not Apoptosis during Alveogenesis

In *Hoxa5*$^{-/-}$ postnatal lungs, proliferation is transiently perturbed while the apoptotic rate remains unchanged. The loss of *Hoxa5* function has been associated with changes in proliferation and/or apoptosis in a number of situations. As for the postnatal lung, in the mammary gland, the pectoral girdle, and the thyroid gland, proliferation but not apoptosis is affected in *Hoxa5* mutants.[51–53] Both processes are diminished in the adult *Hoxa5*$^{-/-}$ stomach.[32] In contrast, ectopic *Hoxa5* expression in the developing spinal cord increases apoptosis without changing proliferation.[54] Finally, *HOXA5* was proposed to control programmed cell death in certain human breast tumor cell lines.[55] Because apoptosis is not influenced by the loss of *Hoxa5* function in the postnatal lung, it is unlikely to contribute to the defective alveogenesis. As for proliferation, the transitory changes observed can explain the lung growth recovery, but it remains to be determined how these variations impact on lung alveogenesis. However, it cannot be excluded that inflammation may influence the proliferative response during this period. Nonetheless, *Hoxa5* involvement in the regulation of proliferation and apoptosis most likely depends on the tissue-specific context and will require further examina-

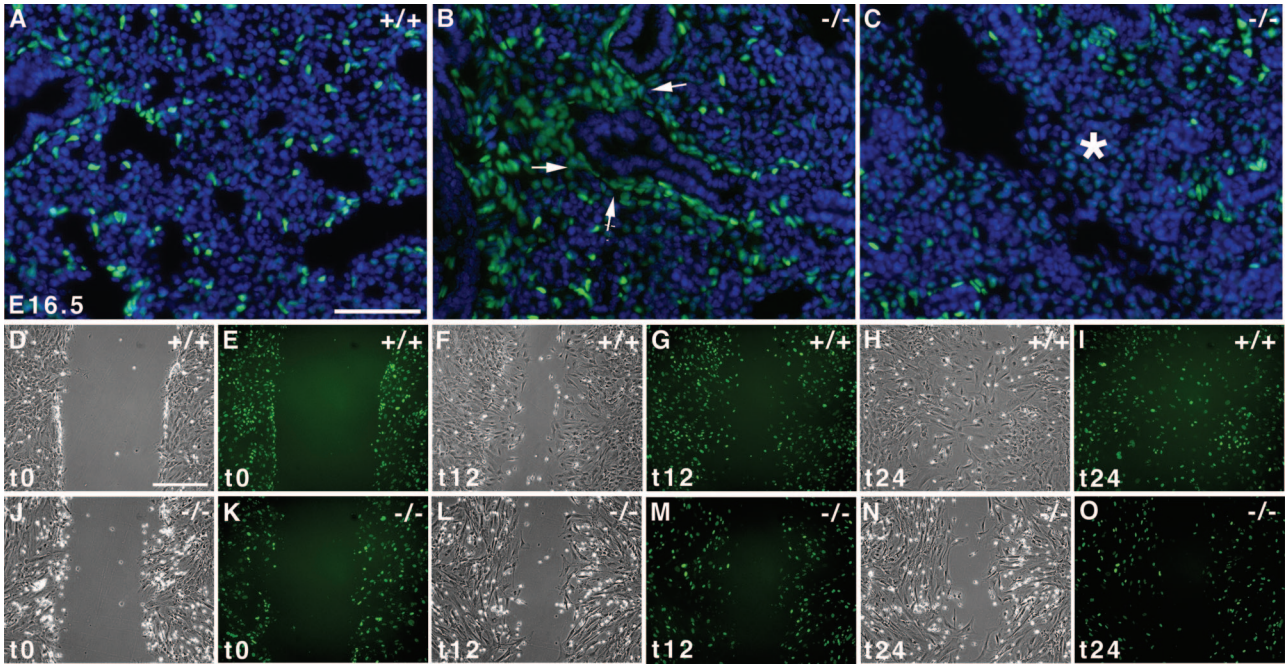

Figure 8. Defective motility of alveolar myofibroblast progenitors. **A–C:** Visualization of the GFP-positive alveolar myofibroblasts progenitors in E16.5 wild-type lungs showed that progenitors were dispersed in the lung parenchyma (**A**). In contrast, most *Pdgfαr/GFP*-positive cells remained clustered around the epithelium in *Hoxa5*$^{-/-}$ lungs, indicating a block in distal spreading of the alveolar myofibroblast progenitors (**B**, **arrows**). Progenitors also failed to invade some lung regions (**C**, **asterisk**). Sections were counterstained with DAPI in blue. **D–O:** Wounding assays of primary mesenchymal cells isolated from lungs of E15.5 *Hoxa5*$^{+/+}$;*Pdgfαr*$^{GFP/+}$ (**D–I**) and *Hoxa5*$^{-/-}$;*Pdgfαr*$^{GFP/+}$ (**J–O**) embryos after 0 (t0; **D**, **E**, **J**, **K**), 12 (t12; **F**, **G**, **L**, **M**), and 24 hours (t24; **H**, **I**, **N**, **O**). Wild-type cells invaded the wounded area within 12 hours of the assay (**F**, **G**), filling the gap by t24 (**H**, **I**). In contrast *Hoxa5*$^{-/-}$;*Pdgfαr*$^{GFP/+}$ cells showed reduced migration at both time points (**L–O**). Scale bars = 50 μm.

tion to dissect its participation in these basic cellular processes.

Contribution of Altered Cell Specification to Impaired Alveogenesis in Hoxa5$^{-/-}$ *Mutants*

Altered cellular specification is consistently observed in tissues affected by the *Hoxa5* mutation.[32,51,53] In the lung, goblet cells and alveolar myofibroblasts are affected by the loss of *Hoxa5* function. The overabundance of mucus-producing cells is a common feature of the *Hoxa5* mutant lung, stomach, and colon phenotypes, suggesting that *Hoxa5* may serve a particular function in their differentiation.[32] The specific ablation of *Foxa2* in the lung epithelium also results in goblet cell hyperplasia and defective alveogenesis without affecting lung morphology before birth.[18] In E12.5 *Hoxa5*$^{-/-}$ lungs, *Foxa2* expression is diminished, whereas in postnatal mutant lungs, the Foxa2 protein is normally detected.[27] The latter observation suggests that abnormal alveogenesis seen in *Hoxa5*$^{-/-}$ lungs is a Foxa2-independent process. However, we cannot rule out the possibility that early perturbations in *Foxa2* expression in the embryonic lung may have late repercussions and contribute to the *Hoxa5*$^{-/-}$ postnatal lung phenotype.

Goblet cell hyperplasia could result from lung inflammation.[4] However, the presence of ectopic goblet cells secondary to an inflammatory stimulus is unlikely because the number of goblet cells is already increased in *Hoxa5*$^{-/-}$ fetal lung specimens before any macrophage recruitment (not shown). The prenatal accumulation of goblet cells rather supports the view that altered proximodistal patterning occurs in the *Hoxa5*$^{-/-}$ respiratory tract. Indeed goblet cells, which are normally restricted to the trachea and primary bronchi, are now ectopically found in more distal structures, like secondary bronchi and bronchioles. In support of this, *Hoxa5* participates in the regionalization of the gut and its mutation causes the stomach to adopt intestinal-like characteristics.[32] Other experimental data, such as the presence of ectopic cartilage in distal *Hoxa5*$^{-/-}$ lungs and the reduced pulmonary branching, also strengthen the hypothesis of perturbed proximodistal patterning of the lung (J.A. and L.J., unpublished).[27] Altogether, these observations are in accordance with the expected role of *Hox* genes in providing essential cues to pattern the respiratory tract.

Alveolar myofibroblasts are also affected by the loss of *Hoxa5* function. The postnatal lung phenotype of *Hoxa5*$^{-/-}$ mutants bears some similarities with that of *Pdgfa*$^{-/-}$ mutants including emphysema morphology and atelectasis.[7,11,28] However, the etiology of impaired alveogenesis in *Hoxa5* mutants differs from that of *Pdgfa*$^{-/-}$ mice. Alveolar myofibroblasts are lacking in *Pdgfa*$^{-/-}$ lungs, whereas they are mispositioned in *Hoxa5*$^{-/-}$ postnatal lungs. Their disappearance in the *Pdgfa*$^{-/-}$ strain, attributable to a block in proliferation and distal spreading, results in reduced elastic fiber deposition and progression to an emphysematous morphology. In *Hoxa5*$^{-/-}$ lungs, alveolar myofibroblasts are rather trapped in the parenchyma where they produce abnor-

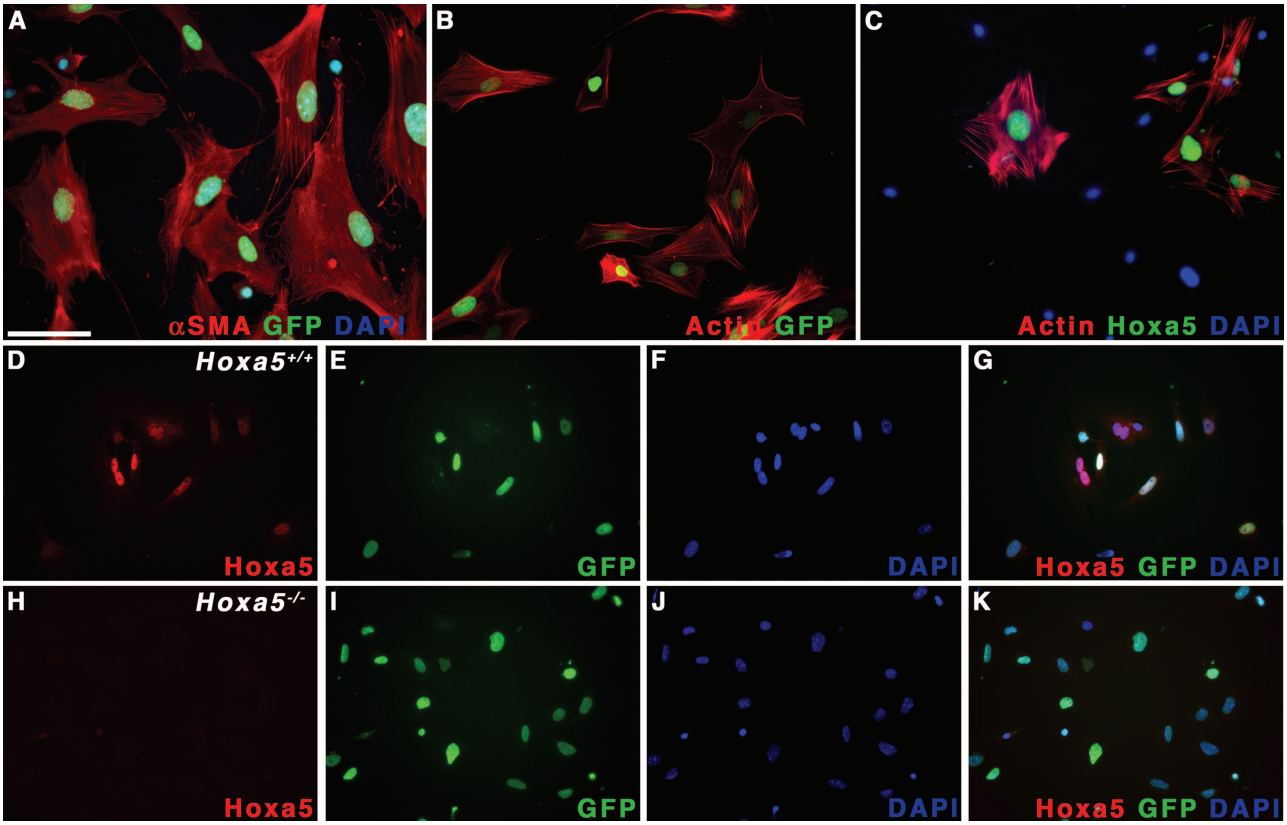

Figure 9. Hoxa5 protein detection in primary embryonic lung myofibroblasts. **A:** Mesenchymal cells isolated from E15.5 lungs adopted a myofibroblast phenotype as shown by the co-expression of Pdgf-α receptor/GFP and α-SMA. **B:** The actin staining observed with phalloidin was identical to that of α-SMA in GFP-positive cells. **C** and **D:** The Hoxa5 protein was readily detected in the nucleus of wild-type myofibroblasts. **D**, **E**, and **G:** Furthermore, GFP and Hoxa5 protein fluorescence extensively overlapped in this cell population. **H–K:** The Hoxa5 protein was not detected in *Hoxa5*$^{-/-}$ cell cultures. Nuclei were counterstained with DAPI (**A**, **C**, **F**, **G**, **J**, **K**). Scale bar = 100 μm.

mal elastic fibers. Nonetheless, *Pdgfa*$^{-/-}$ and *Hoxa5*$^{-/-}$ lungs share a common defect: the subset of mesenchymal cells from which alveolar myofibroblasts originate and that expresses the *Pdgfα* receptor fails to spread into the distal fetal lung. Because *Hoxa5* expression in myofibroblasts extensively overlaps with that of the *Pdgfα* receptor, this supports the notion that *Hoxa5* acts cell autonomously to participate in the specification of this cell population and to influence its motility.

According to the wounding assays, *Hoxa5* affects the capacity of alveolar myofibroblast progenitors to correctly progress to their appropriate position in the lung parenchyma. In Boyden chamber assays, the absence of *Hoxa5* function does not impact on the migratory behavior suggesting that *Hoxa5*$^{-/-}$ lung primary mesenchymal cells can properly respond to gelatin. *Hox* gene involvement in migration has been previously described for endothelial cells and keratinocytes in wound healing *in vivo*.[41,56] The Pdgfa-Pdgfαr signaling network is known to provide appropriate guiding cues that ascertain septa formation.[11,13] It is tempting to speculate that *Hoxa5* regulates *Pdgfαr* gene expression because both genes are co-expressed in the lung myofibroblasts. On the other hand, *Hoxa5* may influence the outcome of Pdgf signaling. Both alternatives are not mutually exclusive and further characterization of the *Hoxa5*$^{-/-}$ lung phenotype should help to decipher this question. Altogether, these results strengthen the notion that proper specification and positioning of the alveolar myofibroblast cell population during embryonic life is critical to ensure proper alveogenesis after birth. They also identify a role for *Hoxa5* in cell motility.

Contribution of Inflammatory Stimuli to Alveolar Defects in Hoxa5$^{-/-}$ *Mutants*

The increased presence of inflammatory cells in *Hoxa5*$^{-/-}$ lungs raises questions about the cause of their accumulation and their contribution to the pathological features of the lung architecture. Although in genetic mouse models of emphysema, alveolar remodeling is progressive and related to the activation of alveolar macrophages and inflammation rather than developmental abnormalities,[57] the lack of alveoli formation in *Hoxa5*$^{-/-}$ lungs favors the view that the inflammatory response is secondary to developmental defects. In *Hoxa5* mutants, activated macrophages are abundantly found in the lung as early as birth and most of them express MMP12. This recruitment coincides with the abnormal elastin deposition by the mispositioned alveolar myofibroblasts. Elastin fragments are chemotactic for monocytes,[49] thus supporting the notion that macrophages accumulate in response to this

cue. The presence of abundant activated macrophages in *Hoxa5*$^{-/-}$ lungs also correlates with a modest increase in MMP activity. In turn, this activity may generate a positive feedback loop that can perpetuate macrophage accumulation, thereby contributing to a chronic inflammatory condition.

Likewise, whereas goblet cell hyperplasia are generally observed under inflammatory conditions,[4,45] the accumulation of goblet cells arises before birth in *Hoxa5*$^{-/-}$ lungs, and thus precedes any sign of inflammation. This favors the view that misspecification of goblet cells may contribute to inflammation. The onset of mucin MUC5AC production at P15, a marker specific for inflammatory conditions in mouse and human chronic lung diseases endorses the chronic inflammation affecting the *Hoxa5*$^{-/-}$ lungs.[18,45]

In summary, the altered cell specification resulting from the *Hoxa5* mutation causes ectopic and hyperplastic goblet cells, and abnormal positioning of myofibroblasts in the postnatal lung, both factors contributing to chronic physiopathological features of the mutant lungs. The lack of formation of alveolar walls precludes the examination of the contribution of the chronic inflammation to the remodeling of the *Hoxa5*$^{-/-}$ lungs. Nonetheless, these results exemplify the importance of genetic contributions to pulmonary diseases. Understanding how *Hoxa5* warrants proper normal lung development should therefore shed light on the etiology of chronic lung pathologies.

Relevance of Hox Genes to Pulmonary Diseases

The respiratory dynamics rely on the viscous and elastic properties within lung parenchyma. Any alteration of surfactant or elastic fibers can jeopardize normal pulmonary function. *Hoxa5*$^{-/-}$ mutants adapt their respiratory behavior and present a modified breathing pattern to compensate for the emphysematous morphology.[28] When parameters of respiratory mechanics are measured in *Hoxa5*$^{-/-}$ mutants, they reveal a decreased lung hysterisivity, a species-independent constant corresponding to the ratio between resistance and elastance of alveolar parenchyma (not shown).[58] The change in hysterisivity in *Hoxa5*$^{-/-}$ mutants reflects the structural lung anomalies.

The *Hoxa5* mutant phenotype shares similarities, without fulfilling all characteristics, of COPD, the sixth most common cause of death worldwide in 1990 that is predicted to become third by 2020.[5] Yet, COPD has been relatively neglected in research on its cellular and molecular mechanisms. Environmental factors such as cigarette smoking are known to affect the susceptibility to develop COPD but genetic factors also contribute, including the inherited deficiency in α_1-antitrypsin, the primary inhibitor of neutrophil elastase, and MMPs that have been identified as key players in lung remodeling in both humans and mice.[49,59–63] In addition, most patients with COPD exhibit airway mucus hypersecretion and goblet cell hyperplasia that may, in a certain subsets of these patients, contribute to morbidity and mortality.[4] Although the emphysema-like architecture of the *Hoxa5*$^{-/-}$ lung does not result from a structural remodeling and destruction of the alveoli with a postnatal onset, understanding the process of normal lung development is crucial for devising strategies to restore normal lung architecture and function in emphysema and lung homeostasis.[64]

Until recently, indirect evidence pinpoints to a potential role of *Hox* genes in alveogenesis as downstream effectors of the therapeutic action of retinoic acid for premature infants.[65] *Hoxa5* might represent one of these important effectors. Moreover, patients suffering from primary pulmonary hypertension and emphysema have augmented and decreased pulmonary *HOXA5* expression, respectively, demonstrating the necessity of proper levels of *Hoxa5* expression in the adult lung.[30] The present work corroborates the notion that altered *Hox* gene expression may predispose to lung pathologies. The study of the cellular and molecular mechanisms underlying the pathological characteristics observed in *Hoxa5*$^{-/-}$ mice may provide significant insights that can translate into better therapeutic strategies.

Acknowledgments

We thank M. Lemieux for careful care of the mouse colony; F. Harel for the statistical analyses; Drs. G. Singh and S. Ho for providing the CC10 and MUC5AC antibodies, respectively; Dr. E. Petitclerc for the HT1080 conditioned media and advice; Dr. P. Soriano for the *Pdgfαr* mouse line; Dr. E. Davis for the mouse tropoelastin probe; and Dr. J. Hogg for insightful comments at the initial stages of this project.

References

1. Perl A-K, Whitsett JA: Molecular mechanisms controlling lung morphogenesis. Clin Genet 1999, 56:14–27
2. Cardoso WV: Lung morphogenesis revisited: old facts, current ideas. Dev Dyn 2000, 219:121–130
3. Warburton D, Schwarz M, Tefft D, Flores-Delgado G, Anderson KD, Cardoso WV: The molecular basis of lung morphogenesis. Mech Dev 2000, 15:55–81
4. Rogers DF: Mucus hypersecretion in chronic obstructive pulmonary disease. Chronic obstructive pulmonary disease: pathogenesis to treatment. Novartis Symposium 2001, 234:65–83
5. Barnes PJ: Small airways in COPD. N Engl J Med 2004, 350:2635–2637
6. Snider GL: Emphysema: the first two centuries—and beyond. A historical overview, with suggestions for future. Am Rev Respir Dis Res 1992, 146:1334–1344
7. Boström H, Willetts K, Pekny M, Levéen P, Lindahl P, Hedstrand H, Pekna M, Hellström M, Gebre-Medhin S, Schalling M, Nilsson M, Kurland S, Törnell J, Heath JK, Betsholtz C: PDGF-A signaling is a critical event in lung alveolar myofibroblast development and alveogenesis. Cell 1996, 85:863–873
8. Noguchi A, Reddy R, Kursar JD, Parks WC, Mecham RP: Smooth muscle isoactin and elastin in fetal bovine lung. Exp Lung Res 1989, 4:537–552
9. Betsholtz C, Karlsson L, Lindahl P: Developmental roles of platelet-derived growth factors. Bioessays 2001, 23:494–507
10. Midwood KS, Schwarzbauer JE: Elastic fibers; building bridges between cells and their matrix. Curr Biol 2002, 12:279–281
11. Lindahl P, Karlsson L, Hellström M, Gebre-Medhin S, Willetts K, Heath

JK, Betsholtz C: Alveogenesis failure in PDGF-A deficient mice is coupled to lack of distal spreading of alveolar smooth muscle cell progenitors during lung development. Development 1997, 124:3943–3953
12. Wendel DP, Taylor DG, Albertine KH, Keating MT, Li DY: Impaired distal airway development in mice lacking elastin. Am J Respir Cell Mol Biol 2000, 23:320–326
13. Prodhan P, Kinane TB: Developmental paradigms in terminal lung development. Bioessays 2002, 24:1052–1059
14. Cardoso WV: Transcription factors and pattern formation in the developing lung. Am J Physiol 1995, 13:429–442
15. Okubo T, Knoepfler PS, Eisenman RN, Hogan BL: Nmyc plays an essential role during lung development as a dosage sensitive regulator of progenitor cell proliferation and differentiation. Development 2005, 132:1363–1374
16. Ikeda K, Shaw-White JR, Wert SE, Whitsett JA: Hepatocyte nuclear factor 3 activates transcription of thyroid transcription factor 1 in respiratory epithelial cells. Mol Cell Biol 1996, 16:3626–3636
17. Bohinski RJ, Di Lauro R, Whitsett JA: The lung-specific surfactant protein B gene promoter is a target for thyroid transcription factor 1 and hepatocyte nuclear factor 3, indicating common factors for organ-specific gene expression along the foregut axis. Mol Cell Biol 1994, 14:5671–5681
18. Wan H, Kaestner KH, Ang S-L, Ikegami M, Finkelman FD, Stahlman MT, Fulkerson PC, Rothenberg ME, Whitsett JA: Foxa2 regulates alveogenesis and goblet cell hyperplasia. Development 2004, 131:953–964
19. Aubin J, Jeannotte L: Implication des gènes Hox dans les processus d'organogenèse chez les mammifères. French. Médecine/Sciences 2001, 17:54–62
20. Takahashi Y, Hamada J, Murakawa K, Takada M, Tada M, Nogami I, Hayashi N, Nakamori S, Monden M, Miyamoto M, Katoh H, Moriuchi T: Expression profiles of 39 HOX genes in normal human adult organs and anaplastic thyroid cancer cell lines by quantitative real-time RT-PCR system. Exp Cell Res 2004, 293:144–153
21. del Toro ED, Borday V, Davenne M, Neun R, Rijli FM, Champagnat J: Generation of a novel functional neuronal circuit in Hoxa1 mutant mice. J Neurosci 2001, 21:5637–5642
22. Rossel M, Capecchi MR: Mice mutant for both Hoxa1 and Hoxb1 show extensive remodeling of the hindbrain and defects in craniofacial development. Development 1999, 126:5027–5040
23. Chisaka O, Capecchi MR: Regionally restricted developmental defects resulting from targeted disruption of the mouse homeobox gene hox-1.5. Nature 1991, 350:473–479
24. Rancourt DE, Tsuzuki T, Capecchi MR: Genetic interaction between hoxb-5 and hoxb-6 is revealed by nonallelic noncomplementation. Genes Dev 1995, 9:108–122
25. Volpe MV, Vosatka RJ, Nielsen HC: Hoxb-5 control of early airway formation during branching morphogenesis in the developing mouse lung. Biochim Biophys Acta 2000, 1475:337–345
26. Volpe MV, Pham L, Lessin M, Ralston SJ, Bhan I, Cutz E, Nielsen HC: Expression of Hoxb-5 during human lung development and in congenital lung malformations. Birth Defects Res 2003, 67:550–556
27. Aubin J, Lemieux M, Tremblay M, Bérard J, Jeannotte L: Early postnatal lethality in Hoxa-5 mutant mice is attributable to respiratory tract defects. Dev Biol 1997, 192:432–445
28. Kinkead R, LeBlanc M, Gulemetova R, Lalancette-Hebert M, Lemieux M, Mandeville I, Jeannotte L: Respiratory adaptations to lung morphological defects in adult mice lacking Hoxa5 gene function. Pediatr Res 2004, 56:553–562
29. Jeannotte L, Lemieux M, Charron J, Poirier F, Robertson EJ: Specification of axial identity in the mouse: role of the Hoxa-5 (Hox1.3) gene. Genes Dev 1993, 7:2085–2096
30. Golpon HA, Geraci MW, Moore MD, Miller HL, Miller GJ, Tuder RM, Voelkel NF: HOX genes in human lung. Altered expression in primary pulmonary hypertension and emphysema. Am J Pathol 2001, 158:955–966
31. Hamilton TG, Klinghoffer RA, Corrin PD, Soriano P: Evolutionary divergence of platelet-derived growth factor alpha receptor signaling mechanisms. Mol Cell Biol 2003, 11:4013–4025
32. Aubin J, Déry U, Lemieux M, Chailler P, Jeannotte L: Stomach regional specification requires Hoxa5-driven mesenchymal-epithelial signaling. Development 2002, 129:4075–4087
33. Giroux S, Charron J: Defective development of the embryonic liver in N-myc-deficient mice. Dev Biol 1998, 195:16–28
34. Vachon E, Bourbonnais Y, Bingle CD, Rowe SJ, Janelle M-F, Tremblay GM: Anti-inflammatory effect of pre-elafin in lipopolysaccharide-induced acute lung inflammation. Biol Chem 2002, 383:1249–1256
35. Wert SE, Yoshida M, LeVine AM, Ikegami M, Jones T, Ross GF, Fisher JH, Korfhagen TR, Whitsett JA: Increased metalloproteinase activity, oxidant production, and emphysema in surfactant protein D gene-inactivated mice. Proc Natl Acad Sci USA 2000, 97:5972–5977
36. Sato T, Koike L, Miyata Y, Hirata M, Mimaki Y, Sashida Y, Yano M, Ito A: Inhibition of activator protein-1 binding activity and phosphatidylinositol 3-kinase pathway by nobiletin, a polymethoxy flavonoid, results in augmentation of tissue inhibitor of metalloproteinases-1 production and suppression of production of matrix metalloproteinases-1 and -9 in human fibrosarcoma HT-1080 cells. Cancer Res 2002, 62:1025–1029
37. Yang Y, Palmer KC, Relan N, Diglio C, Schuger L: Role of laminin polymerization at the epithelial mesenchymal interface in bronchial myogenesis. Development 1998, 125:2621–2629
38. Mailleux AA, Kelly R, Veltmaat JM, De Langhe SP, Zaffran S, Thiery JP, Bellusci S: Fgf10 expression identifies parabronchial smooth muscle cell progenitors and is required for their entry into the smooth muscle cell lineage. Development 2005, 132:2157–2166
39. Tétreault M-P, Chailler P, Rivard N, Ménard D: Differential growth factor induction and modulation of human gastric epithelial regeneration. Exp Cell Res 2005, 306:285–297
40. Le Boeuf F, Houle F, Huot J: Regulation of vascular endothelial growth factor receptor 2-mediated phosphorylation of focal adhesion kinase by heat shock protein 90 and Scr kinase activities. J Biol Chem 2004, 279:39175–39185
41. Hansen SL, Myers CA, Charboneau A, Young DM, Boudreau N: HoxD3 accelerates wound healing in diabetic mice. Am J Pathol 2003, 163:2421–2431
42. Joksimovic M, Jeannotte L, Tuggle CK: Dynamic expression of murine HOXA5 protein in the central nervous system. Gene Express Patt 2005, 5:792–800
43. Littell RC, Henry PR, Ammerman CB: Statistical analysis of repeated measures data using SAS procedures. J Anim Sci 1998, 76:1216–1231
44. Kresch MJ, Christian C, Wu F, Hussain N: Ontogeny of apoptosis during lung development. Pediatr Res 1998, 43:426–431
45. Borchers MT, Wert SE, Leikauf GD: Acrolein-induced MUC5ac expression in rat airways. Am J Physiol 1998, 274:573–581
46. Mariani TJ, Reed JJ, Shapiro SD: Expression profiling of the developing mouse lung. Insights into the establishment of the extracellular matrix. Am J Respir Cell Mol Biol 2002, 26:541–548
47. Jostarndt-Fögen K, Djonov V, Draeger A: Expression of smooth muscle markers in the developing murine lung: potential contractile properties and lineal descent. Histochem Cell Biol 1998, 110:273–284
48. Chung KF: Cytokines in chronic obstructive pulmonary disease. Eur Respir J 2001, 18:50–59
49. Parks WC, Shapiro SD: Matrix metalloproteinases in lung biology. Respir Res 2001, 2:10–19
50. Aubin J, Chailler P, Ménard D, Jeannotte L: Loss of Hoxa5 gene function in mice perturbs intestinal maturation. Am J Physiol 1999, 277:C965–C973
51. Garin É, Lemieux M, Coulombe Y, Robinson GW, Jeannotte L: Stromal Hoxa5 function controls the growth and differentiation of mammary alveolar epithelium. Dev Dyn 2006, 235:1858–1871
52. Aubin J, Lemieux M, Moreau J, Lapointe J, Jeannotte L: Cooperation of Hoxa5 and Pax1 genes during formation of the pectoral girdle. Dev Biol 2002, 244:96–133
53. Meunier D, Aubin J, Jeannotte L: Perturbed thyroid morphology and transient hypothyroidism symptoms in Hoxa5 mutant mice. Dev Dyn 2003, 227:367–378
54. Abbott MA, Joksimovic M, Tuggle CK: Ectopic HOXA5 expression results in abnormal differentiation, migration and p53-independent cell death of superficial dorsal horn neurons. Dev Brain Res 2005, 159:87–97
55. Chen H, Chung S, Sukumar S: HOXA5-induced apoptosis in breast cancer cells is mediated by caspases 2 and 8. Mol Cell Biol 2004, 24:924–935

56. Mace KA, Hansen SL, Myers C, Young DM, Boudreau N: HOXA3 induces cell migration in endothelial and epithelial cells promoting angiogenesis and wound repair. J Cell Sci 2005, 118:2567–2577
57. Brusselle GG, Bracke KR, Maes T, D'hulst AI, Moerloose KB, Joos GF, Pauwels RA: Murine models of COPD. Pulm Pharmacol Ther 2006, 19:155–165
58. Fredberg JJ, Stamenovic D: On the imperfect elasticity of lung tissue. J Appl Physiol 1989, 67:2408–2419
59. Laurel C-B, Ericsson S: The electrophoretic α1-globulin pattern of serum in α1-antitrypsin deficiency. Scand J Clin Lab Invest 1963, 15:132–140
60. Hautamaki RD, Kobayashi DK, Senior RM, Shapiro SD: Requirement for macrophage elastase for cigarette smoke-induced emphysema. Science 1997, 277:2002–2004
61. Russell RE, Thorley A, Culpitt SV, Dodd S, Donnelly LE, Demattos C, Fitzgerald M, Barnes PJ: Alveolar macrophage-mediated elastolysis: roles of matrix metalloproteinases, cysteine, and serine proteases. Am J Physiol 2002, 283:867–873
62. DeMeo DL, Silverman EK: Alpha1-antitrypsin deficiency. 2: Genetic aspects of alpha(1) antitrypsin deficiency: phenotypes and genetic modifiers of emphysema risk. Thorax 2004, 59:259–264
63. Foronjy RF, Okada Y, Cole R, D'Armiento J: Progressive adult-onset emphysema in transgenic mice expressing human MMP-1 in the lung. Am J Physiol 2003, 284:727–737
64. Mahadeva R, Shapiro SD: Chronic obstructive pulmonary disease #3: experimental animal models of pulmonary emphysema. Thorax 2002, 57:908–914
65. Chinoy MR, Nielsen HC, Volpe MV: Mesenchymal nuclear transcription factors in nitrogen-induced hypoplastic lung. J Surg Res 2002, 108:203–211